

## Diffusion of the Silicon Dimer on Si(001): New Possibilities at 450 K

Brian Borovsky, Michael Krueger, and Eric Ganz

*Department of Physics, University of Minnesota, Minneapolis, Minnesota 55455*

(Received 6 December 1996)

We report on the discovery of a novel diffusion pathway for silicon dimers on the Si(001) surface. As a small molecule, the dimer's configuration can play a central role in its diffusion. Using scanning tunneling microscopy movies at temperatures near 450 K, we show, in real time, changes in the dimer's configuration during its diffusion. These changes in configuration provide a pathway for diffusion *across* the substrate dimer rows, unlike the well-known diffusion along the dimer rows. The important energies involved in dimer row crossing are measured. [S0031-9007(97)03274-2]

PACS numbers: 68.35.Fx, 07.79.Cz, 61.16.Ch

Over the past few decades, powerful techniques for imaging with atomic resolution have provided a unique look at the complex and sometimes surprising motion of atomic species on surfaces [1–7]. When the diffusing species is a molecule of two or more atoms, several different orientations of the molecule relative to the substrate may be involved, resulting in unique forms of diffusion. In this Letter, we discuss new scanning tunneling microscopy (STM) experiments which reveal a novel form of diffusion by a simple molecule, the Si dimer, on the Si(001) surface. The Si(001) surface is the basis for most lithographic and nanofabrication methods, and has been the subject of intensive experimental and theoretical investigations. The growth of Si on Si(001) has been widely used as a model system in the study of the fundamental processes in the homoepitaxial growth of crystals. Surface diffusion plays an essential role in such processes. Si dimers adsorbed on the Si(001) surface have recently been the subject of careful study, particularly at the relatively low temperatures from room temperature up to 400 K [8–14]. Several experiments have demonstrated that dimers readily form on the surface, are very stable, and may play an important role in the initial stages of epitaxial growth [15–17]. Experiments have also shown that dimer diffusion is highly anisotropic, with the dimer diffusing primarily along the tops of dimer rows [14,15]. *Ab initio* calculations by both Yamasaki *et al.* and Brocks *et al.* have emphasized the significance of dimers, finding that no additional activation energy to the diffusion barrier of a monomer is required to form the dimer, and that once formed the dimer is stable, with a lower energy per atom than monomers [11,13].

Experimental and theoretical evidence suggests that there are four principal dimer configurations on Si(001). As shown in Fig. 1, a dimer can sit on top of a dimer row (A and B) or in the trough between two rows (C and D), with its axis oriented either parallel or perpendicular to the dimer row direction. (Figure 2 shows a STM image of a dimer adsorbed on top of a dimer row at 360 K.) All four configurations have been identified in STM experiments [8–10,16,17]. Theoretical calculations of the energies of

these configurations have been subjects of controversy over the last several years [8,11,12,17]. However, STM observations have firmly established that configuration B is higher in energy than configuration A [8,10,17]. A recent measurement of this energy difference by Swartzentruber *et al.* found that B is higher by  $59 \pm 9$  meV [8]. Consistent with these experiments, recent *ab initio* calculations by Yamasaki *et al.* place configuration A lowest in energy, followed by B, C, and D, with relative energies 0, 80, 180, and 760 meV, respectively [11].

Our experiments on Si dimers are performed using a custom STM which is capable of imaging at elevated temperatures. It is housed in an ultrahigh vacuum chamber with a base pressure of  $5 \times 10^{-11}$  torr. The samples are prepared by flashing to 1250 °C for 30 seconds. They are then transferred to the STM stage and allowed to equilibrate overnight at the desired temperature between 300 and 450 K. A small amount of material (<0.01 ML) is subsequently deposited onto the surface from a resistively heated Si wafer. The well-known dimer diffusion along the tops of the dimer rows was observed and its rate was calibrated, as a function of temperature, in a separate experiment using atom tracking [14,18]. The sample temperature is found by measuring the dimer hop rate with atom tracking and using this calibration.

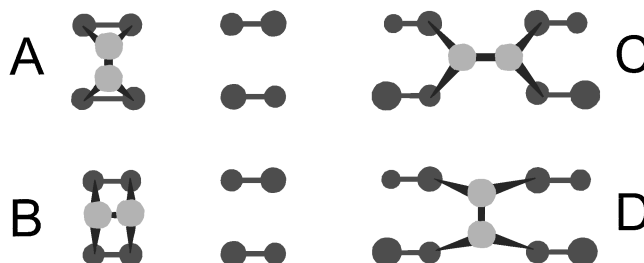


FIG. 1. Schematic drawings of the configurations of isolated adsorbed dimers on Si(001), after Brocks and Kelly [12]. Black circles represent substrate atoms. Gray circles represent adatoms on the surface. Lines are drawn to indicate the electronic bonds. Segments of four substrate dimer rows are shown in the figure, running vertically.

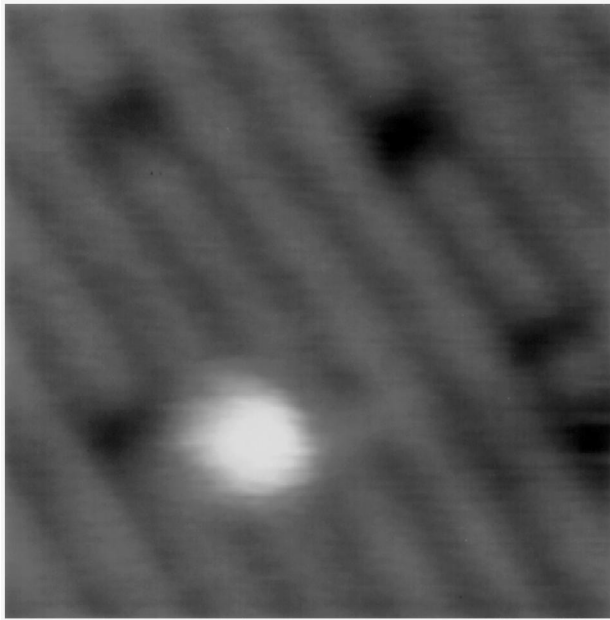


FIG. 2. A  $65 \text{ \AA} \times 65 \text{ \AA}$  STM image at 360 K showing a dimer adsorbed on top of a dimer row. The rows are diagonal in the image. Since dimers readily rotate between configurations A and B at this temperature, the resulting image is a mixture of the two. This is a filled-state image, with sample bias  $= -2.0 \text{ V}$ .

At temperatures near 450 K, we observe that dimers are able to diffuse across the dimer rows of the substrate. At these temperatures, dimers diffuse along the tops of dimer rows very rapidly, hopping at a rate of about 10 Hz. This activity is easily visible in hot STM movies, as shown in Fig. 3(a). The rapidly diffusing dimer is trapped between two surface defects and appears as a blur along the dimer row. This image took 20 seconds to scan, so the dimer repeatedly occupied many different positions along the dimer row during acquisition of the image, giving the dimer its blurred appearance. We find that the dimer is occasionally able to convert to a configuration centered on the trough between two rows and marked by two lobes, one on each of the neighboring rows, as shown in Fig. 3(b). In this configuration the dimer appears so faint that it is often nearly invisible to the STM, leading to its designation as the “stealth dimer.” The dimer diffuses much more slowly in this configuration, as evidenced by its well-defined position in the image. But by Fig. 3(c), 20 seconds later, it has clearly moved ahead of its previous position. In Fig. 3(d), the dimer is again diffusing rapidly; however, it is located on the top of the row next to the original one. [The original row is marked with an arrow in Fig. 3(a) and Fig. 3(d).] Figure 3 thus demonstrates a mechanism for dimer diffusion across the dimer rows. This row crossing process is not observed at temperatures below 450 K. As described below, we are able to identify the stealth dimer as a type C dimer, but neither conversion to this configuration nor diffusion of a type C dimer has yet been reported.

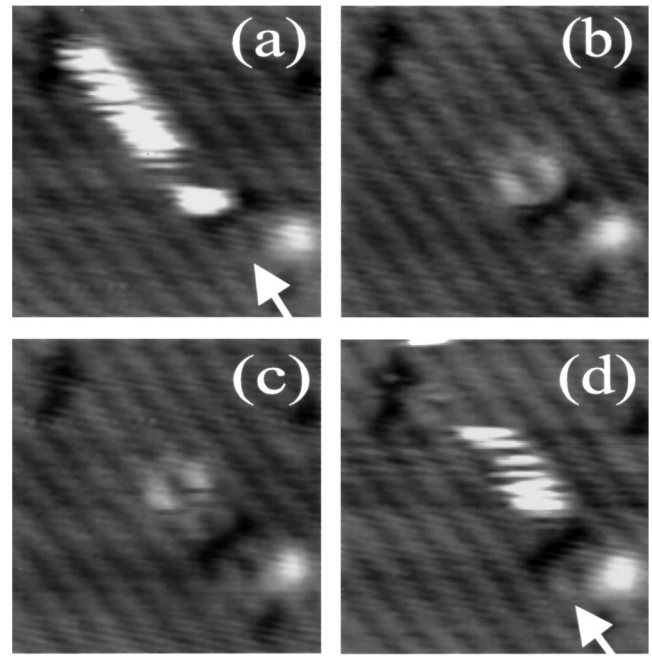


FIG. 3. A sequence of  $130 \text{ \AA} \times 130 \text{ \AA}$  STM images at 450 K showing dimer diffusion across dimer rows. The arrows in images (a) and (d) point to the same dimer row. In image (a), the dimer (white streak) is moving rapidly on top of this row. Its motion is bounded by two surface defects. Images (b) and (c) show slower diffusion in the intermediate stealth dimer state (faint twin lobes), which is a type C dimer. In image (d), the dimer reappears on top of an adjacent row. These are filled-state images, with sample bias  $= -2.0 \text{ V}$ .

Crucial to the interpretation of the stealth dimer configuration is the local density of states (LDOS) calculation of Brocks and Kelly [12]. This calculation shows that a filled-state STM image of the type C dimer will be dominated by the dangling bonds of two surface atoms, one on each of the neighboring rows. This explains the two-lobed appearance of the dimer shown in the filled-state images of Fig. 3(b) and 3(c). Comparison with our own room temperature filled-state and empty-state images and those of van Wingerden *et al.* further confirms the identification [10].

Based on several hot STM movie sequences depicting diffusion across dimer rows, at  $450 \pm 5 \text{ K}$ , we are able to estimate the relevant energies. In the following analysis, we have used four movie sequences, which follow 5 dimers through a total of 27 conversions to or from the C configuration. For the dimers observed, the average residence time on top of a row was  $675 \pm 151 \text{ sec}$ . The average residence time in the trough was  $116 \pm 20 \text{ sec}$ . These results indicate that the C configuration is less stable than one or both of the configurations on top of the dimer row. Using a simple “Boltzmann factor” analysis, we may obtain the energy of C relative to the lowest-energy configuration, A, without knowledge of the detailed pathway involved in the conversion process. When

the dimer is on top of a dimer row, it rotates between configurations A and B. According to the results of Swartzentruber, at 450 K we expect this rotation to occur with a frequency of over 1 kHz, with the dimer spending 82% of its time in the A configuration [8]. For each conversion event, the dimer therefore spends an average total time of  $\tau_A = 0.82 \times (675 \pm 151 \text{ sec}) = 554 \pm 124 \text{ sec}$  in the A configuration,  $\tau_B = 0.18 \times (675 \pm 151 \text{ sec}) = 121 \pm 27 \text{ sec}$  in the B configuration, and (as given above)  $\tau_C = 116 \times 20 \text{ sec}$  in the C configuration. Ratios of these times give the relative populations of A, B, and C, which, in equilibrium, are governed by the Boltzmann factor,  $e^{-\Delta E/kT}$ . Here  $\Delta E$  is the energy difference between two states,  $k$  is the Boltzmann constant, and  $T$  is the temperature. We find that the C configuration is  $61 \pm 16 \text{ meV}$  higher in energy than A. This value is substantially lower than that arrived at in recent *ab initio* calculations [11,12]. However, we confirm the *ab initio* theoretical prediction that configuration A is lower in energy than C [11,12], in contrast to the empirical potential result, which reverses this ordering [17].

The activation energies for leaving the trough and for diffusion in the C configuration may be obtained through the Arrhenius relation, which gives the rate of a thermally activated process:  $r = 1/\tau = \nu e^{-E/kT}$ . Here  $r$  is the rate, or the reciprocal of the average residence time  $\tau$ . The activation energy and prefactor for the process are  $E$  and  $\nu$ , respectively. (Recently, we measured the activation energy and prefactor for dimer diffusion along the top of a dimer row, using atom tracking [18]. We found a value of  $1.09 \pm 0.05 \text{ eV}$  for the activation energy, with a prefactor of  $10^{13.2 \pm 0.6} \text{ Hz}$ . For consistency, we will use our measured prefactor in the following analysis, noting that this measured value is typical of what one would expect for these processes [19].) Using the average residence time in the trough given above, we find a value of  $1.36 \pm 0.06 \text{ eV}$  for the energy barrier to leaving the trough. According to the diffusion pathway proposed below, we interpret this as the energy barrier to entering the B configuration from C. We observe an average hop rate in the trough of  $0.4 \pm 0.2 \text{ Hz}$  at 450 K. The Arrhenius relation yields a barrier to diffusion in the trough of  $1.21 \pm 0.09 \text{ eV}$ .

We propose the following diffusion pathway for row crossing, shown schematically in Fig. 4 along with a plot depicting the energies involved. Since configuration C is perpendicular to the lowest-energy configuration, A, diffusion across dimer rows requires rotation of the dimer. Such rotation has been both predicted and observed to occur on top of the dimer rows, between configurations A and B [8,9,16,17]. Therefore, it is natural to propose that the dimer jumps from the B configuration directly to C. We do not believe the pathway involves the D configuration since its energy is calculated to be significantly higher than A, B, or C [11,12]. We have also considered an alternative mechanism for conversion

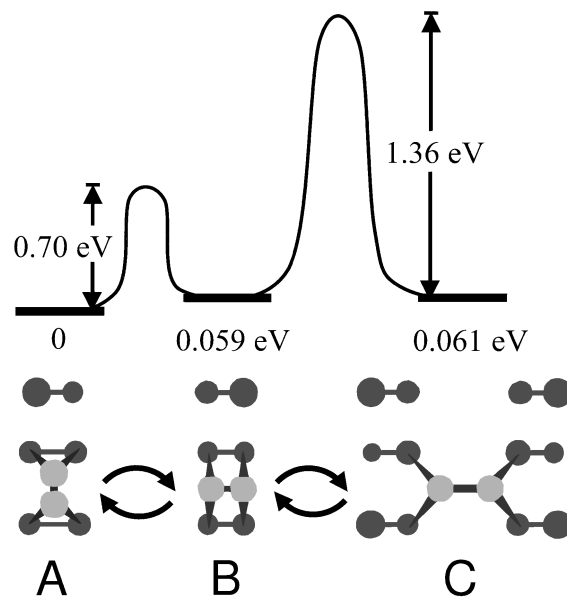


FIG. 4. A schematic diagram of the proposed diffusion pathway for row crossing, along with a graphical depiction of the important energies involved. The dimer rotates from A to B as it diffuses along the top of a dimer row. Occasionally, the dimer may jump from B to C, overcoming an energy barrier of  $1.36 \pm 0.06 \text{ eV}$ . The dimer then diffuses along the trough, or may jump to the top of either neighboring dimer row. We measure the binding energy of C to be  $0.061 \pm 0.016 \text{ eV}$  relative to A. According to the results of Swartzentruber, B has an energy of  $0.059 \pm 0.009 \text{ eV}$  relative to A, and the barrier from A to B is  $0.70 \pm 0.08 \text{ eV}$  [8].

to the C configuration, in which the dimer on top of a row dissociates into two monomers, which then join again to form a dimer in the C configuration. Recent results in our lab show that, using atom tracking in empty-state conditions (positive sample bias), the dimer can be continuously tracked as it moves into the C configuration. No hops longer than one lattice spacing are observed in the tracking data. We therefore conclude that dissociation is not responsible for dimer diffusion across dimer rows. Thus we propose the pathway A-B-C for dimer diffusion across dimer rows. It should be feasible to test this pathway with current theoretical methods.

The diffusion of dimers across dimer rows may have important implications for the homoepitaxial growth of Si on Si(001). For growth regimes where there are large numbers of dimers present, we expect the quality of the epitaxial growth process to depend on the area accessible to diffusing dimers prior to being incorporated into the crystal. We have shown that, at a critical threshold near 450 K, dimer diffusion converts from one dimensional to two dimensional, with the onset of diffusion across dimer rows. Below this temperature, dimers are confined to move along single dimer rows between defects and step edges. Above this temperature, dimers are able to escape from these one-dimensional traps and interact with features over a much larger

area. In doing so, we may expect that dimers can not only find favorable epitaxial locations more easily, but also more effectively convert metastable structures into epitaxial structures. Such conversion processes have recently been proposed to be important in low temperature epitaxial growth [12]. Furthermore, it has been proposed that it is the C configuration, and not A or B, which binds additional monomers and promotes one-dimensional growth at low temperatures [11,12], making conversion to the C configuration itself important in understanding epitaxial growth at low temperatures. The interactions of dimers with various metastable and epitaxial structures, dimer-dimer interactions, and the lifetime of dimers on the Si(001) surface are currently being studied in our lab to help clarify the role of dimers in epitaxial growth.

We have investigated the energetics and kinetics of Si dimer diffusion across dimer rows on Si(001). We observe a striking example of a diffusion pathway that involves several distinct dimer configurations. By making use of the STM's atomic scale resolution, one can distinguish between the various configurations accessible to the molecule during its diffusion, allowing detailed interpretation of the diffusion pathway. Future extensions of this technique will incorporate the use of atom tracking to improve the time resolution [14,18]. These investigations could be extended to the study of the surface chemical reaction dynamics important in such processes as chemical vapor deposition and catalysis. As the molecules of interest become more complicated, so do their possible bonding geometries to the substrate. As a result, the number and complexity of available diffusion pathways increases.

We gratefully acknowledge Eric Hill for his assistance. We also thank J. van Wingerden for providing preprints of his work. This research is supported by NSF Grant No. DMR-9222493.

---

[1] G.L. Kellogg and P.J. Feibelman, Phys. Rev. Lett. **64**, 3143 (1990).

- [2] D. W. Bassett and P. R. Webber, Surf. Sci. **70**, 520 (1978).  
[3] J. D. Wrigley and G. Ehrlich, Phys. Rev. Lett. **44**, 661 (1980).  
[4] R. T. Tung and W. R. Graham, Surf. Sci. **97**, 73 (1980).  
[5] D. C. Senft and G. Ehrlich, Phys. Rev. Lett. **74**, 294 (1995).  
[6] E. Ganz, S. K. Theiss, I. Hwang, and J. Golovchenko, Phys. Rev. Lett. **68**, 1567 (1992).  
[7] S. J. Stranick, A. N. Parikh, D. L. Allara, and P. S. Weiss, J. Phys. Chem. **98**, 11 136 (1994).  
[8] B. S. Swartzentruber, A. P. Smith, and H. Jónsson, Phys. Rev. Lett. **77**, 2518 (1996).  
[9] A. van Dam, J. van Wingerden, M. J. Haye, P. M. L. O. Scholte, and F. Tuinstra, Phys. Rev. B **54**, 1557 (1996).  
[10] J. van Wingerden, A. van Dam, M. J. Haye, P. M. L. O. Scholte, and F. Tuinstra, Phys. Rev. B **55**, 4723 (1997).  
[11] T. Yamasaki, T. Uda, and K. Terakura, Phys. Rev. Lett. **76**, 2949 (1996).  
[12] G. Brocks and P. J. Kelly, Phys. Rev. Lett. **76**, 2362 (1996).  
[13] G. Brocks and P. J. Kelly, and R. Car, Surf. Sci. **269/270**, 860 (1992).  
[14] B. S. Swartzentruber, Phys. Rev. Lett. **76**, 459 (1996). Atom tracking is a technique in which the STM tip is locked onto the top of a substrate feature using lateral feedback electronics, so that each diffusive event is resolved.  
[15] D. Dijkamp, E. J. van Loenen, and H. B. Elswijk, in *Proceedings of the 3rd NEC Symposium on Fundamental Approach to New Material Phases*, Springer Series on Material Science (Springer-Verlag, Berlin, 1992).  
[16] P. J. Bedrossian, Phys. Rev. Lett. **74**, 3648 (1995).  
[17] Z. Zhang, F. Wu, H. J. W. Zandvliet, B. Poelsema, H. Metiu, and M. G. Lagally, Phys. Rev. Lett. **74**, 3644 (1995).  
[18] M. Krueger, B. Borovsky, and E. Ganz, Surf. Sci. (to be published). Additional information is available at our web site (<http://www.physics.umn.edu/groups/stmlab>).  
[19] D. Srivastava and B. J. Garrison, Phys. Rev. B **47**, 4464 (1993).